Journal of Mining and Earth Sciences

Website: https://jmes.humg.edu.vn

Determination of borders of structure related to deep minerals based on potential field data in Ba Na area

Hong Thi Phan [1,*], Thong Duy Kieu [1], Phuong Minh Do[2], Huu Van Tran [1]

[1] *Hanoi University of Mining and Geology, Hanoi, Vietnam*
[2] *The Vietnam Geological Department, Hanoi, Vietnam*

ARTICLE INFO

Article history:
Received 08th Nov. 2023
Revised 28th Feb. 2024
Accepted 15th July 2024

Keywords:
Ba Na,
COSCAD-3D,
Energy filter,
Live window,
Potential field,
Statistics.

ABSTRACT

This paper presents the research results of applying method two-dimensional energy filtering method in the «live window» to separate the high-frequency component of aeromagnetic data in order to eliminate residual flight line errors with amplitude ranges from -5÷5 nT and correct the data source before processing and analysis of data, identify potential field residual anomalies at depths h = 470 m, 1100 m, 1700 m, 2300 m. Application of the horizontal gradient of the vertical derivative of the potential field at various depths to determine the position of shallow fault systems, and determine the boundaries of local heterogeneous blocks related to the prospect of deep-hidden minerals at depths h = 470 m, 1100 m, 1700 m, 2300 m in Ba Na area. The results of the analysis of residual magnetic anomalies have built the distribution diagram of the shallow fault system buried by sediments and zoning the mineral prospect according to the potential anomaly in the study area. Fault system includes faults in sub-latitude, sub-longitude, and Northeast-Southwest directions, in which the sub-latitude fault system is dominant. The area of mineral prospect in Ba Na area to a depth h = 2300 m is determined by the maximum value of horizontal gradient vertical derivative of the closed loop residual gravity anomaly field with amplitude >0.007 mGal/m², combined with residual gravity anomaly value, and location of mineral points have been revealed on the surface, prospective areas are mainly concentrated in the west, northwest, and southeast of the study area. The results of the analysis provided Geophysicists and Geologists with detailed research plans to evaluate specific types of minerals in the Ba Na area.

*Corresponding author.
E-mail phanthihong@humg.edu.vn
DOI: 10.46326/JMES.2024.65(4).06

1. Introduction

The study area (Ba Na - Hoi An area) is elongated in the sub-latitude direction and is limited by two deep faults, namely the Cu De river fault (north) and the Vu Gia river fault (south). At the same time, in the area occurs complex intrusive magmatic activities that enrich and diversify the petrographic composition, extending from the Proterozoic to the Cenozoic. This tectonic activity is a favourable geological premise for the formation of endogenous mineral deposits (such as Au, Fe, Mo, W, molybdenite, and other metals) (Nguyen, 2000a; 2000b; 2014) and they have been revealed on the topographic surface (Figure 1b). These geological structure features are all represented by different residual densities and residual magnetic induction values, which are shown on the potential field values measured on the observed surface (or in the air) (Figure 2).

Boundaries of geological structures or shallow fault systems are analyzed using the method of horizontal gradient vertical derivative anomaly of potential field (Nguyen et al., 2014). It is easy to see that residual anomalies greatly affect the accuracy of the above calculation. In previous studies, the residual anomaly field was calculated as the sum anomaly field minus the anomaly field when using energy filters at different «fixed window» sizes (Geosoft, 2008; http://www.

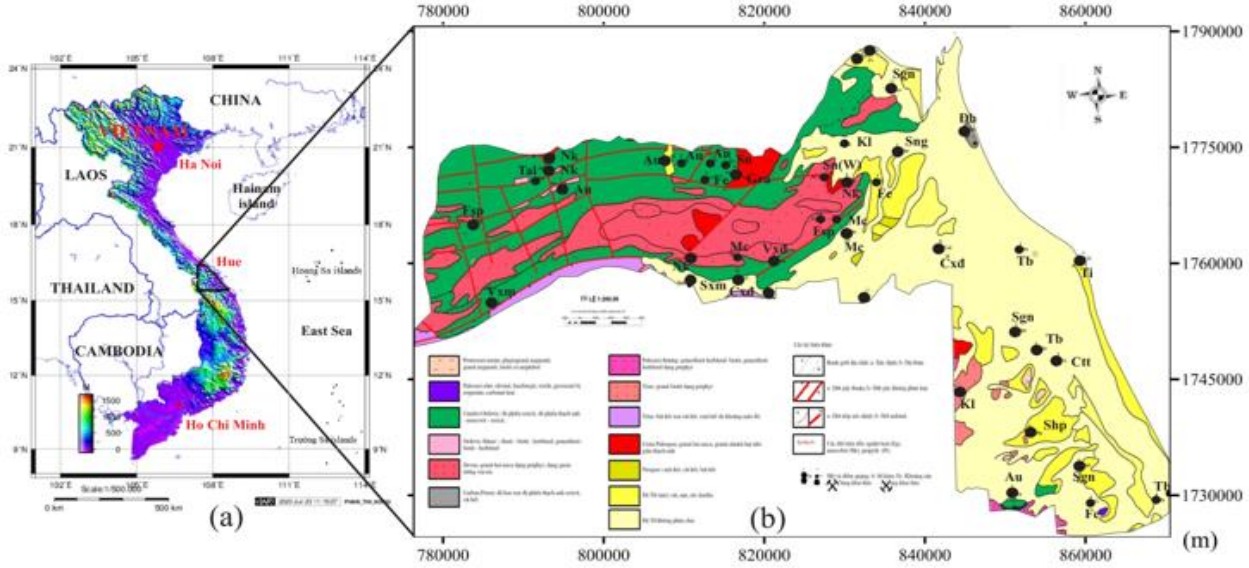

Figure 1. Location of the study area (Ba Na area), terrain elevation above mean sea level varies from 10 ÷1200 m (https://topex.ucsd.edu) (a); Geological map of the study area (reduced from scale 1:200 000) (b).

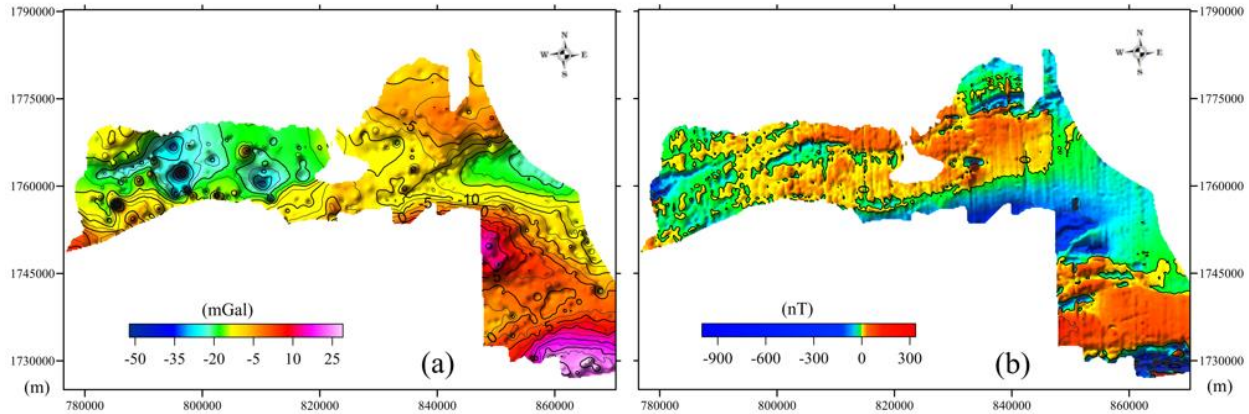

Figure 2. Map of full Bughe gravity anomalous field at scale 1:100 000, distance between two isovals is 2.5 mGal (a); Map of the aeromagnetic anomalous field at scale 1:200 000, the distance between the two isovals is 100 nT in Ba Na area (b).

geosoft.com; https://www.generic mapping-tools.org). This result will lose or distort the local anomaly field information, leading to highly skewed processing results. To optimize this result, we study and apply «live window» form energy filters with different sizes to separate the residual field anomalies at different depths (http://www.coscad3d.ru; Nikitin and Petrov, 2008; Petrov et al., 2010; Petrov, 2018; Nikitin et al., 2006; Phan et al., 2021; Hong et al., 2021). The advantage of the method is that at each window size of the filter, the autocorrelation function will be calculated to evaluate the correlation direction that coincides with the anomaly direction using the most energy, and then the filter window shape will be selected according to the field's correlation radius. This filtering method has improved the accuracy and minimized the loss or distortion of the calculated residual anomaly field.

In this paper, we present the results of analyzing potential field anomalies by the «live window» form energy filtering method to determine the residual field anomalies of locally heterogeneous objects to the extent that depth z=2300 m and the method of the maximum horizontal gradient of vertical derivative anomalies of the residual field to locate the shallow fault system and localize prospects related to deep hidden minerals in Ba Na area.

2. Dataset and methodologies

2.1. Dataset

The data sources used in the article include the Bughe gravity anomaly field data at the scale of 1:100 000 (Nguyen, 2000a; 2000b) measured on the ground after adjusting the altitude, adjusting the middle layer with density δ_{lg} = 2.67 g/cm^3 and terrain correction by method Prisivanco L. N (Blakely, 1996) with an accuracy of 0.1÷0.25 mGal. (Figure 2a).

The source of the magnetic anomaly field data at the scale of 1:200 000 (Nguyen, 2000a; 2000b; 2014;), conducted aeromagnetic measurements in the year 2000 with the proton magnetometer MAP-4 with a sensitivity ±1 nT. The magnetic anomalous value ΔT_a is calculated by the total magnetic anomaly field T_{2000} minus the normal magnetic field T_0 in 2000 taken on the IGRF 2000 international standard field map by the Institute of Geophysics of the Center for Natural Sciences and Technology National technology provided (www.ncdc.noaa.gov) (Figure 2b).

Observing the diagram of the Bughe gravity anomaly field (Figure 2a), the anomaly field changes in the range of -60÷30 mGal, dividing 3 main field regions: the western region is characterized by the negative anomaly band -60÷-20 mGal, the central area is characterized by anomalous values with amplitude from -10÷10 mGal, the southeast region is characterized by the highest positive anomaly values from 0÷30 mGal. At the same time, there are many local bulk anomalies in the area.

Observation of the magnetic anomaly field diagram (Figure 2b), the magnetic anomaly field in the area is very noisy with amplitude varying from -1000÷350 nT, which is classified into 3 main areas: the west and northwest characterized by bands of positive anomalies with amplitude from 0÷200 nT extending in the sub-latitude direction and on the background of positive normal anomalies appear many local anomalies with alternating yin and yang amplitudes, and especially in the central part appear pairs alternating yin and yang anomalies with large amplitudes from -500÷350 nT. The Eastern region is characterized by a negative heterojunction with an amplitude of -900÷-100 nT. The southeast region is characterized by a positive anomaly band with amplitudes from 50÷350 nT. There are many local anomalies on the positive anomaly background alternating negative and positive local anomalies with amplitude ranging from -200÷150 nT.

2.2. Methodologies

2.2.1. The method of energy filtering «live window» form

In complex real conditions, the measured potential field anomalies are not caused by an object but are superimposed by anomalies caused by close objects together with deep geological structures, therefore, the separation of the shallow local small-size field related to mineral potential sites from the total anomalous field is performed by us on energy filters at «live window» sizes differently.

At each window size, the autocorrelation function is evaluated to evaluate the direction of correlation coinciding with the attack of the most energy-intensive anomaly. The correlation radius is calculated by the formula (http://www.coscad3d.ru; Nikitin and Petrov, 2008; Petrov et al., 2010; Petrov, 2018; Nikitin et al., 2006; Phan et al., 2021; Hong et al., 2021):

$$R(n,m) = \frac{1}{M-|m|}\cdot\frac{1}{N-|n|}\sum_{j=1}^{M-|m|}\sum_{i=1}^{N-|n|}\left(f_{ij} - \bar{f}\right)\left(f_{i+n,j+m} - \bar{f}\right) \quad (1)$$

Where: f_{ij} - is the value of the observable field; $\bar{f}$ - is the mean field value; N - is the total number of survey points along the ox axis; M - is the total number of survey lines along the oy axis; n, m - are the distance of consecutive values in the ox axis (n = 0, ±Δx, ±2Δx,...) and in the oy axis (m = 0, ±Δy, ±2Δy,...) represents the distance between the field values f_{ij} and $f_{i+n,j+m}$ in the filter window area.

At each window position, the autocorrelation function (Formula 1) will be calculated and according to the experimental results (http://www.coscad3d.ru; Nikitin and Petrov, 2008; Petrov et al., 2010; Petrov, 2018; Nikitin et al., 2006), we will choose the correlation radius R(n, m) ≥ 0.15, so at each window, we will get different filter window shapes, these window shapes are typical for the statistical properties and spectral correlations of the field in the window, illustrated in Figure 3b. The average field value will be calculated in the window area with R(n, m) ≥ 0.15 and assigned the value to the centre point of the filter window.

To see the advantages of the «live window» form energy filter compared to the «fixed window» form energy filter, we surveyed a forward model consisting of a V-block (area field characteristic), 02 small size spheres (local field characteristics) and additional random noise with noise amplitude equal to 0.8 times the maximum anomaly amplitude, it is shown in Figure 3a.

Observing the filter results in Figure 4b (rectangular «fixed window» shape) and Figure 4c («live window» shape) shows:

- The filter results with the rectangular «fixed window» (Figure 4b) distort the two wings of the V-shaped block, and the information of the two spherical local blocks is not visible on the field diagram.

- The filter results with the «live window» (Figure 4c) reflect the information on both wings of the V-block and the two spherical locales. Optimal filtering results in the filtering process, the statistical characteristics and spectral correlation of the survey field are taken into account in the filter window area, according to the correlation radius R(n, m) the shape of the filter window changes continuously (Figure 3b) to adapt to the changing characteristics of the field.

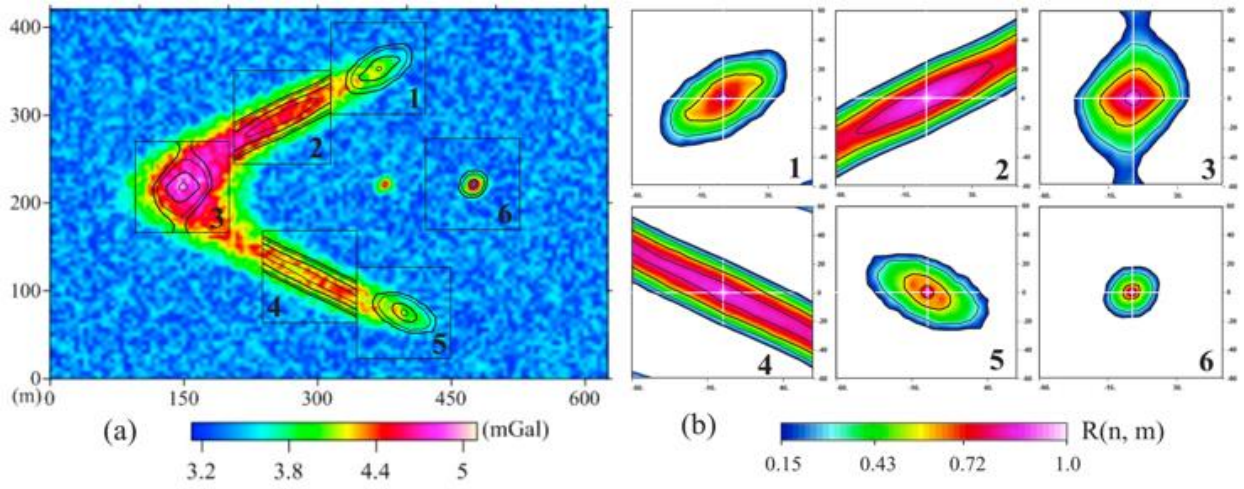

Figure 3. The forward model consists of 01 V-block, 02 spheres with random noise, and a typical filter window position with window size 105×105 m (a); The window shape of the energy filter changes to adapt to the field characteristics at the window positions in Figure 3(a) according to the statistical characteristics and spectral correlation, choosing the correlation radius R(n,m)≥0.15 (b).

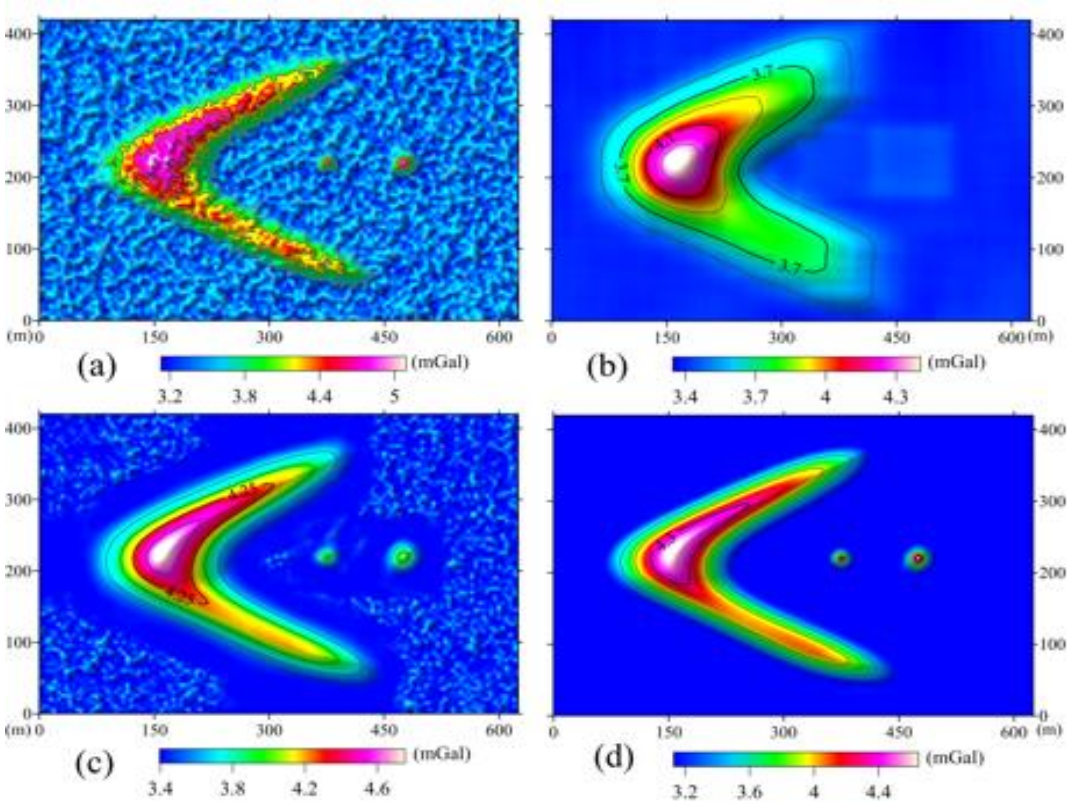

Figure 4. The forward model anomaly contains random noise with noise amplitude equal to 0.8 times the maximum anomaly amplitude (a); Filtering results using an energy filter with a rectangular «fixed window» size of 105×105 m (b); Filtering results using an energy filter with a «live window» size according to Figure 2(b) 105×105 m (c); The forward model anomaly does not contain random noise (d).

Thus, the separation of the field local anomalies related to the deep-hidden mineral location, and the energy filter in the form of a «live window» is the optimal choice. The filter minimizes the loss or distortion of the calculated residual anomaly field. In this paper, for Ba Na area we will perform energy filtering with increasing window sizes (for gravity data: 750×750 m, 1750×1750 m, 2750×2750 m, 3750×3750 m; with aeromagnetic data: 1750×1750 m, 4250×4250 m, 6750×6750 m, 9250×9250 m) to identify local heterogeneous blocks at the respective depths: h = 470 m; 1100 m, 1700 m, 2300 m.

2.2.2. Method of maximum horizontal gradient of potential field vertical derivative.

The method used to determine the boundary of local inhomogeneous blocks related to the deep-hidden mineral location is by the location of the set of horizontal gradient maxima points of the vertical derivative of the potential field (Figure 5). The horizontal gradient maximization method was first applied by Cordell (Cordell, 1979) in determining the boundary of the object according to the position of the points with the maximum value of the horizontal gradient. This method was later developed and applied by the authors to many different regions (Blakely, 1996; Fedi and Florio, 2001; Verduzco et al., 2004; Nguyen et al., 2014).

To improve the resolution of the maximum horizontal gradient method, we apply the maximum horizontal gradient method to the vertical derivative of the potential field. The horizontal gradient amplitude is calculated according to the formula:

$$the\ HD\_VD = \sqrt{\left(\frac{\partial VD}{\partial x}\right) + \left(\frac{\partial VD}{\partial x}\right)} \qquad (2)$$

Where: *VD* is the vertical derivative of the

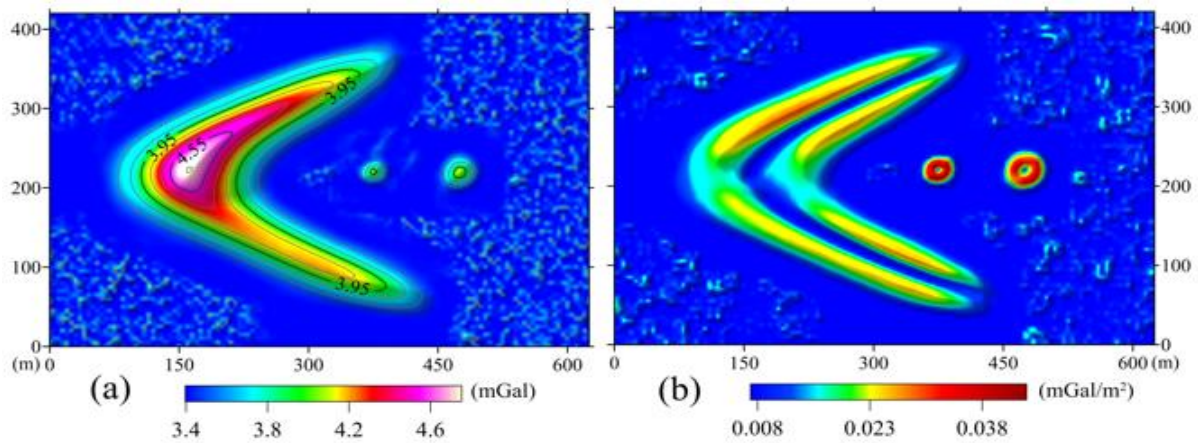

Figure 5. The forward model anomaly contains random noise (a); The result of calculating the horizontal gradient amplitude of the vertical derivative according to formula (2), the set of horizontal gradient maxima values reflects the boundary of the V-shaped and the boundary of two spheres (b).

potential field ($VD = \frac{\partial f(x,y)}{\partial z}$); *x and y* are the directions along the Ox and Oy axes.

3. Results and Discussions

3.1. Results of noise removal due to linear effects and transfer magnetic field to the equator in Ba Na area.

Observing the map of the total aeromagnetic anomaly field (Figure 6a), we observe streaks along the meridian direction, if using this data source directly in the processing in the next steps, it will deform and make errors in processing results. Therefore, in this paper, we use the «live window» energy filtering method to separate the high-frequency component of the magnetic anomaly field, the results (Figure 6b) clearly show the shape of the aviation route during the field survey. The results showed shortcomings in the processing of aeronautical observations, and we gave the appropriate correction value and obtained the results after removing the high-frequency noise caused by the flight path (Figure 6c).

Ba Na area is located at low latitudes, near the equator - where the inclined magnetization and magnetic anomalies have a poor correlation with the geological object causing the anomaly. Therefore, in this paper, we use the method of magnetic transfer to the equator (Figure 6c) on Geosoft software (Geosoft, 2009). This is a new method applied to low magnetic latitudes to correct the position of magnetic anomalies that is the best coincidence with their source, making it easier to interpret anomalies without losing physical meaning.

Figure 6(d) is the result of transferring the aeromagnetic field to the equator of the study area with an inclination angle of I=18.33^0, deviation from D = -0.55^0 determined from the webpage (www.ngdc.noaa.gov) with field measurements in 2000.

3.2. Results of residual anomalies at different depths

The residual anomaly field at the depths is calculated by the sum of the anomaly field minus the anomaly field after filtering the «live window» form energy with different window sizes. For anomaly gravity data, we filter with window sizes (750×750 m, 1750×1750 m, 2750×2750 m, 3750×3750 m), for anomaly magnetic data (1750×1750 m, 4250×4250 m, 6750×6750 m, 9250×9250 m) to identify residual anomalies bearing information of local heterogeneous masses at the respective depths: h = 470 m; 1100 m, 1700 m, 2300 m (Figures 7, 8).

Observing the residual gravity anomaly (Figure 7), the residual magnetic anomaly (Figure 8) we have observed in the west and northwest regions are characterized by many clusters of positive gravitational anomalies with amplitudes from 1÷10 mGal (Figure 7), positive magnetic anomalies extending along the sub-latitude,

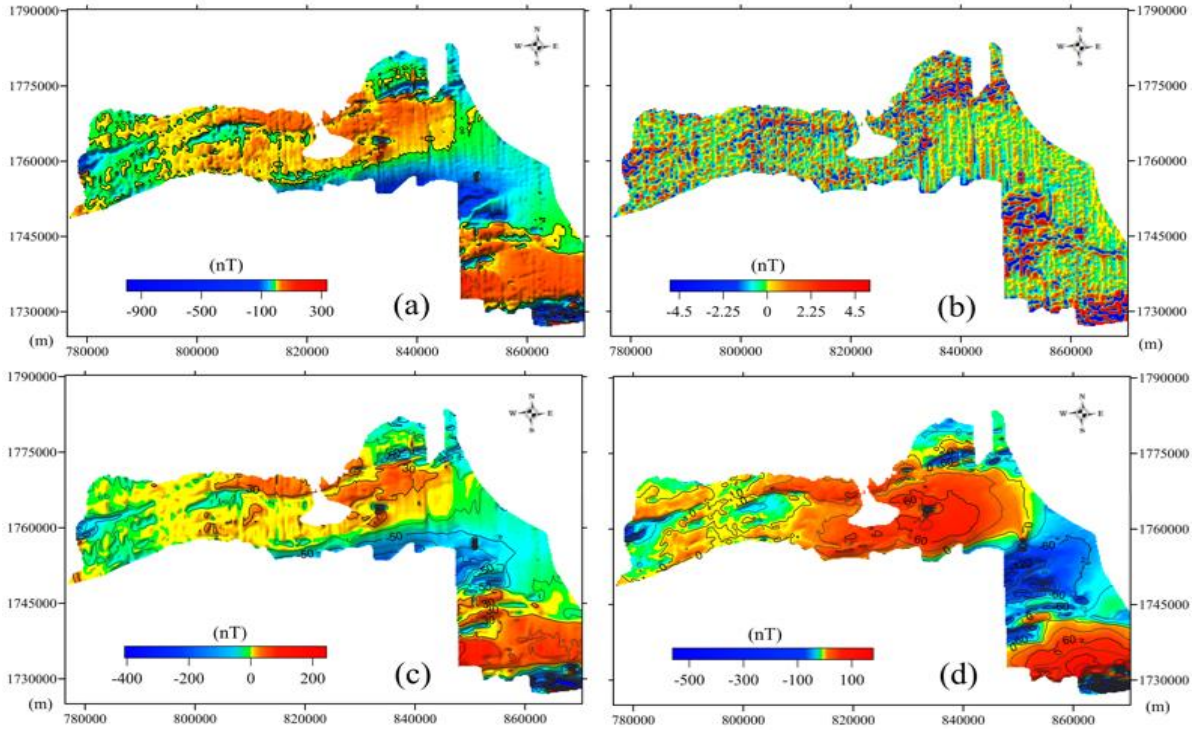

Figure 6. Map of total magnetic anomaly field (a); The noise due to the flight route effect is eliminated by a «live window» energy filter with a window size of 750×750 m (b); Map of magnetic anomaly field after removing noise due to flight route effect in Figures 6(b) (c); Map of magnetic anomaly field moving to the equator in Ba Na area (d).

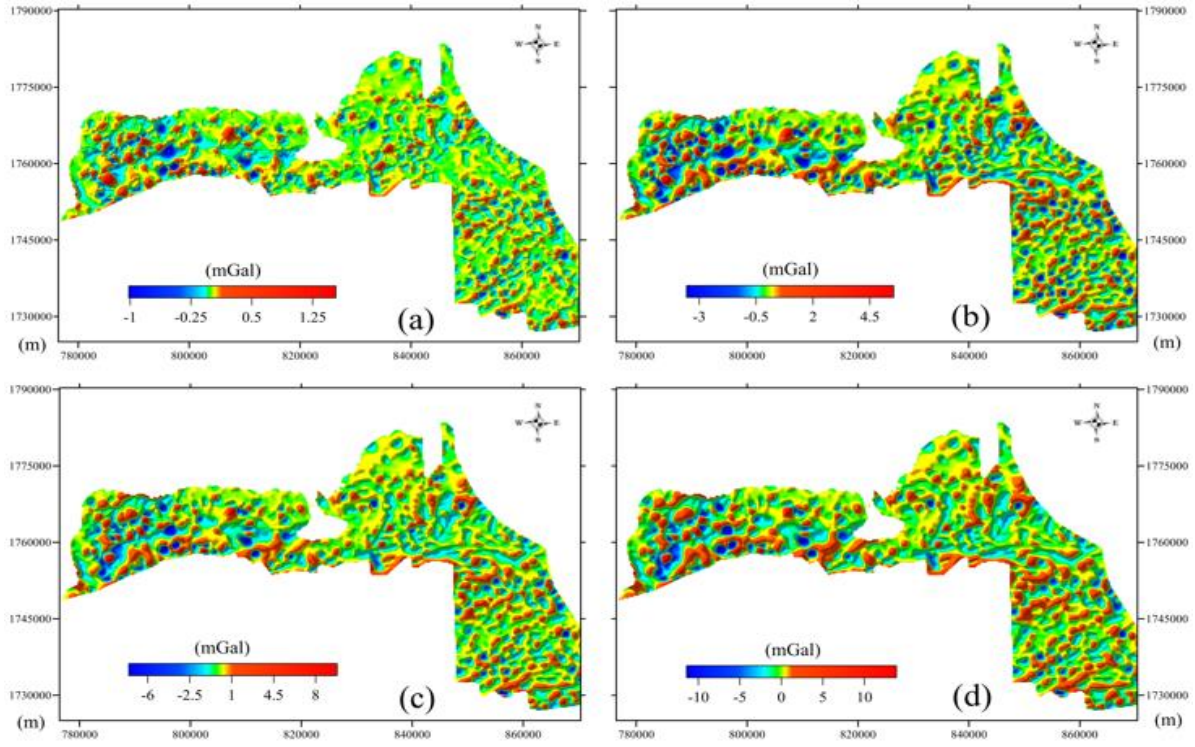

Figure 7. Map of local residual gravity anomalies at depth of h = 470 m (a); at depth of h = 1100 m (b); at depth of h = 1700 m (c); at depth of h = 2300 m (d) Ba Na area.

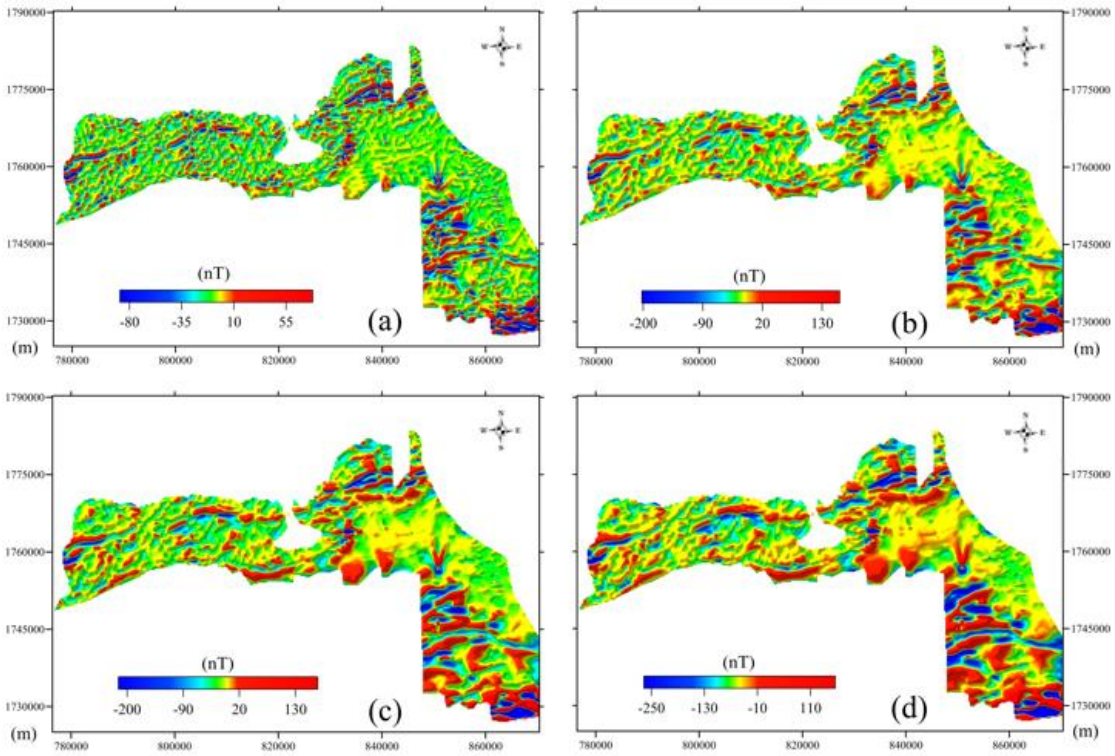

Figure 8. Map of local residual magnetic anomalies at depth of h = 470 m (a); at depth of h = 1100 m (b); at depth of h = 1700 m (c); at depth of h = 2300 m (d) Ba Na area.

and the northwest-southeast with a positive amplitude from 20÷150 nT (Figure 8). The central region is characterized by a strong positive gravity anomaly cluster of 2÷8 mGal, corresponding to pairs of alternating negative and positive magnetic anomalies with a rather large amplitude of -200÷130 nT reflecting the anomalous cluster associated with iron minerals. The Eastern region is characterized by the potential field anomaly with a very small amplitude of change. The southeast region is characterized by many positive gravity anomalies accompanied by alternating pairs of negative and positive magnetic anomalies.

3.3. The results of calculating the horizontal gradient value of the vertical derivative of the potential field.

We calculate the horizontal gradient of the vertical derivative for the potential field local residual anomaly at different depths (Figures 7 and 8) and get the results shown in Figures 9 and 10.

Observing the horizontal gradient value of the vertical derivative of the residual gravity anomaly field (Figure 9), we see that there are many local heterogeneous blocks in the area characterized by the circular closed horizontal gradient maxima band with amplitude >0.07 mGal/m^2. Local heterogeneous blocks are concentrated with quite large density in the west, northwest, and southeast of the study area, which shows that there is a rather complicated disturbance of rock composition here. The Eastern area shows relatively stable soil composition through the value of the horizontal gradient field which does not change significantly. Since the local heterogeneous blocks are very well characterized by the residual density parameter and identified on the residual anomaly values relative to the surrounding rock, therefore, we based on the results of evaluating the horizontal gradient of the residual gravity anomaly at different depths h= 470 m, h=1100 m, h=1700 m, h=2300 m (Figures 9a, b, c, d) together with the locations showing mineral spots in Figure 1(b) to delineate the potential boundaries of deep-hidden minerals in Ba Na area and shown in Figure 9(e). Observing the horizontal gradient value of the vertical derivative of the residual magnetic

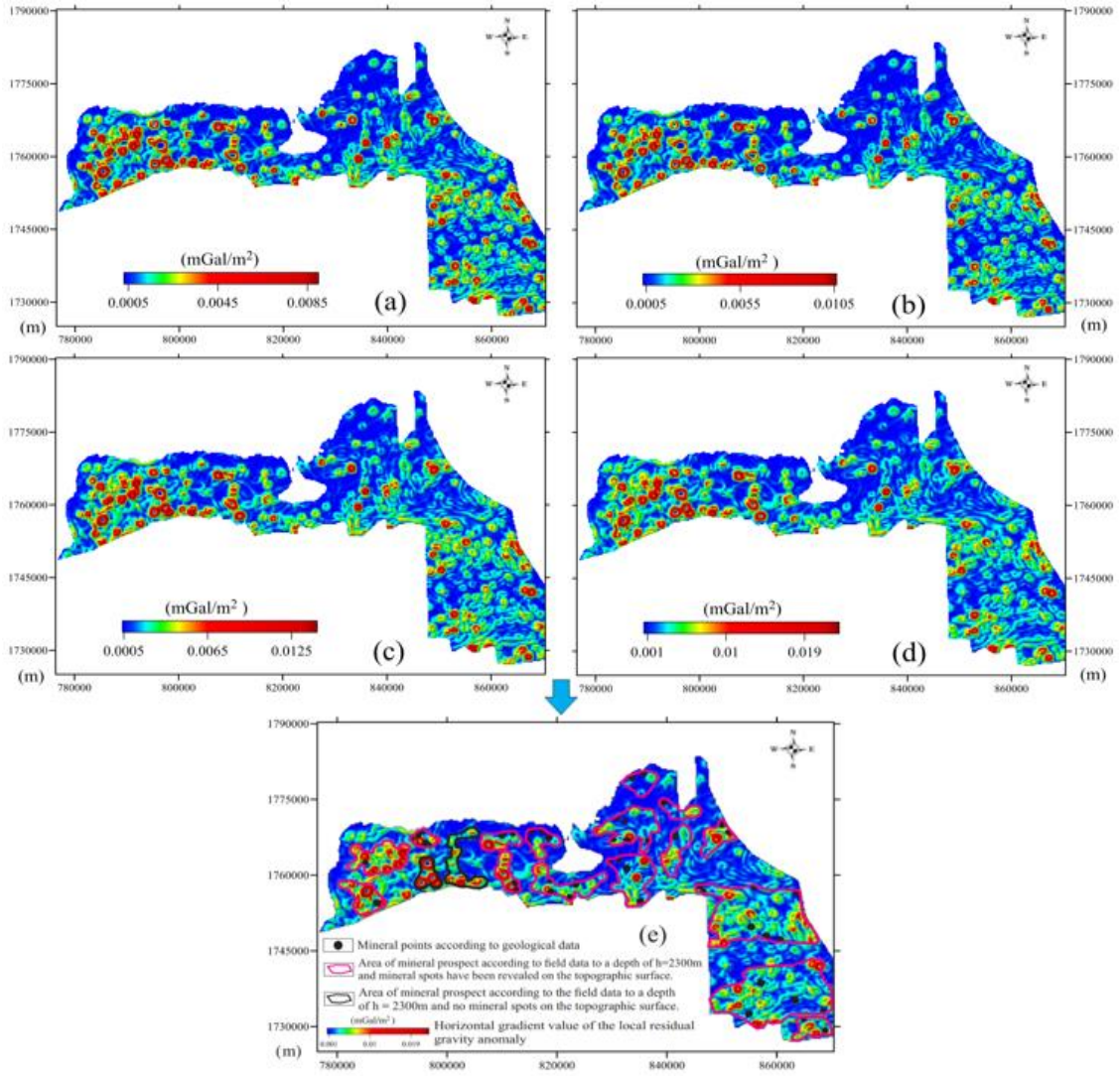

Figure 9. Results of horizontal gradient calculation of the vertical derivative of local residual gravity anomaly at depth of h = 470 m (a); at depth of h = 1100 m (b); at depth of h = 1700 m (c); at depth of h = 2300 m; and Results of identification zoning of potential mineral areas to a depth of z=2300 m according to the analysis of horizontal gradient value of the vertical derivative of local residual gravity anomaly (e) in Ba Na area.

anomaly (Figure 10) shows that the bands of maximum horizontal gradient values extend mainly in the sub-latitude direction and the northwest-southeast.

The west, northwest, and southeast areas are characterized by long horizontal gradient maxima bands with amplitude >0.1 nT/m^2 in the sub-latitude direction, northwest-southeast with relatively thick density, demonstrated at this area has very complex tectonic activities and these are potential areas for forming mineral deposits. The Eastern area is characterized by a small horizontal gradient field <0.05 nT/m^2, showing that the geological activity here is quite stable. The centre of the study area is characterized by a loop-shaped closed horizontal gradient maxima with an amplitude of >0.3 nT/m^2, indicating that this area may have the potential of magma/mineral mass with high magnetic composition.

According to the results of calculating the horizontal gradient value of the vertical derivative of the magnetic anomalous field, the extended horizontal gradient maxima bands characterize the positions of the fault systems. According to the value of horizontal gradient amplitude, we divide into 2 fault levels: the first level fault is characterized by long horizontal gradient maxima

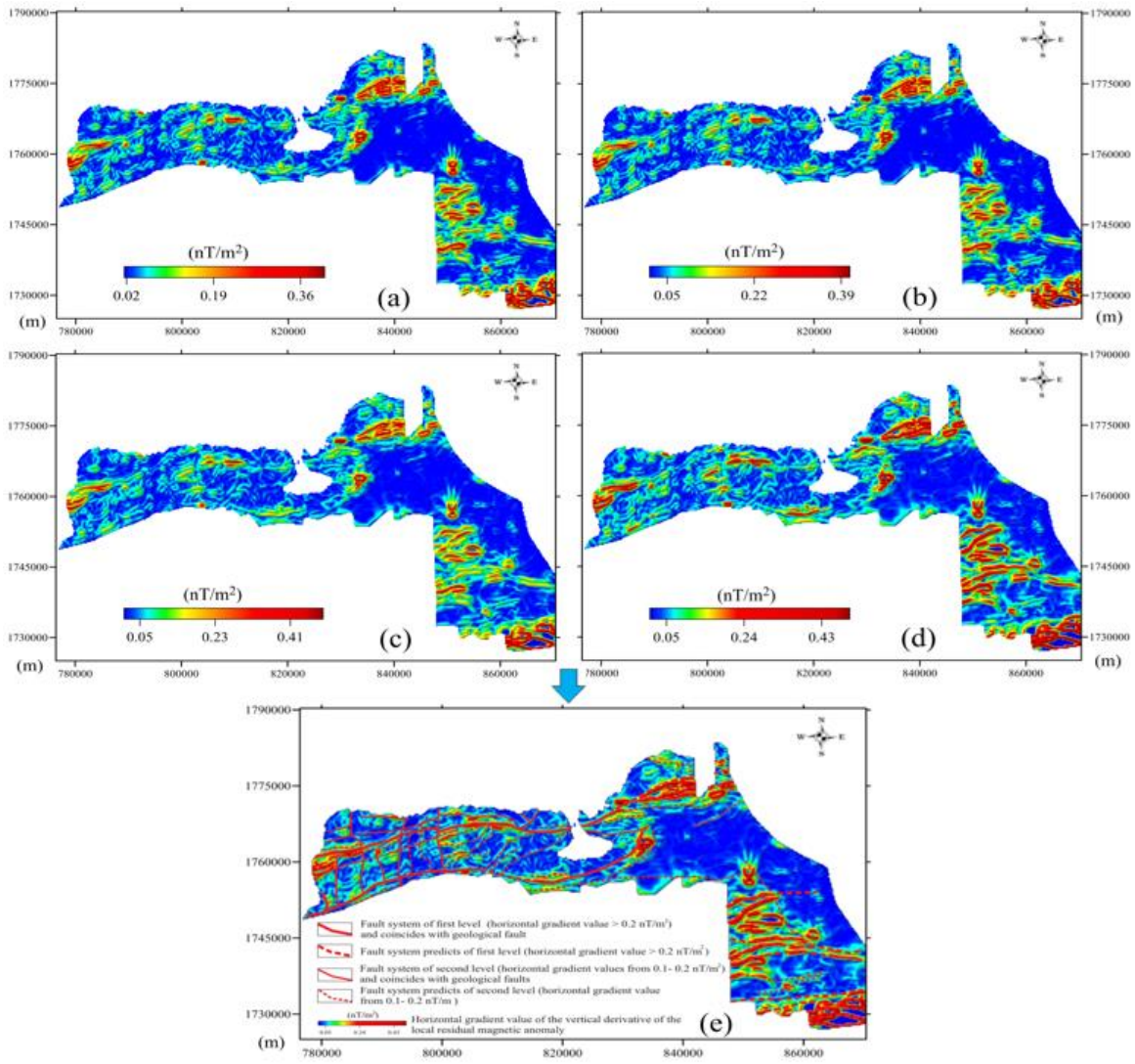

Figure 10. Results of horizontal gradient calculation of the vertical derivative of the local residual magnetic anomaly at depth of h = 470 m (a); at depth of h = 1100 m (b); at depth of h = 1700 m (c); at depth of h = 2300 m (d); and Results of identification of fault systems to a depth of z=2300 m according to the analysis of horizontal gradient value of the vertical derivative of the local residual magnetic anomaly in Ba Na area.

with amplitude >0.2 nT/m²; the secondary fault is characterized by long horizontal gradient maxima ranges with amplitude from 0.1÷0.2 nT/m², and get the results of locating the faults shown in Figure 11(e).

3.4. Results of determining the boundaries of structures related to deep-hidden minerals in the Ba Na area

Summarize the results of identification zoning of potential mineral areas to a depth of z=2300 m according to the analysis of horizontal gradient value of the vertical derivative of local residual gravity anomaly (Figure 9e) and results of identification of fault systems to a depth of z=2300 m according to the analysis of horizontal gradient value of the vertical derivative of the local residual magnetic anomaly (Figure 10e), we have built a diagram of the boundaries of structures related to deep-hidden minerals in the Ba Na area and the results are shown in Figure 11.

Looking at Figure 11 we see in the west of the Ba Na area, the fault system is close to the geological fault (shown by the red solid line), and in the East of the study area, due to the terrain bordering the East Sea, most of the faults are covered by sediment, so according to the

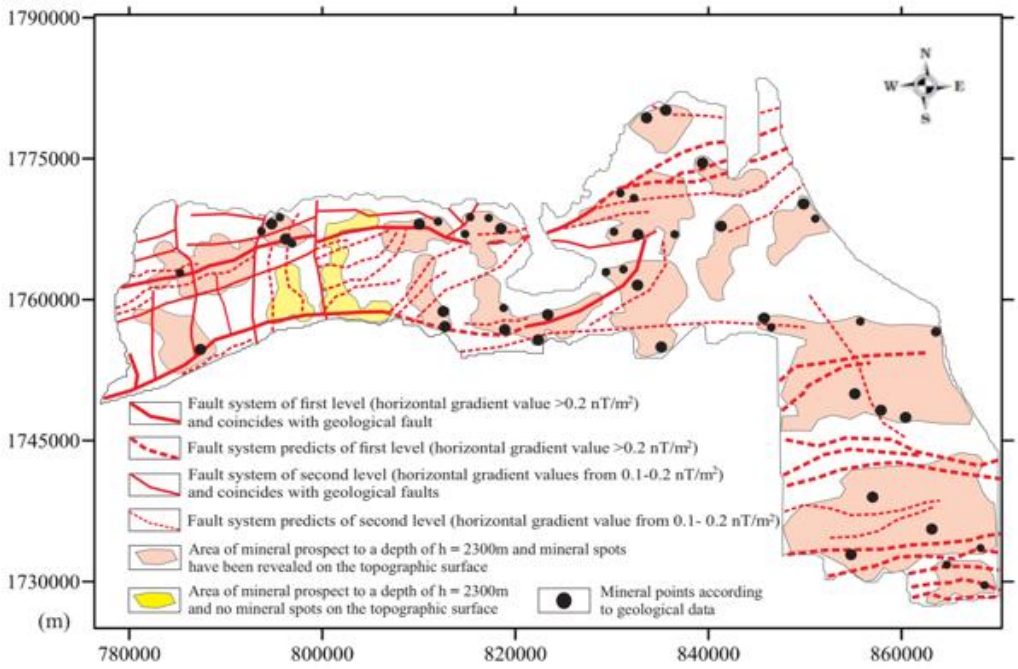

Figure 11. Results of identification of fault systems and zoning of potential mineral areas to a depth of z=2300 m according to the analysis of potential field data in Ba Na area.

geological data (Figure 1), it is almost impossible to locate the faults and with the results of our analysis of the magnetic anomaly data, We identified the locations of these faults. The predicted fault system is shown in Figure 11 (shown by the red dashed line).

The main fault system in the area mainly develops in the sub-latitude direction and the northwest-southeast. The west and northwest regions are characterized by sub-latitude and sub-longitude fault systems, creating complex geological structures, forming structures with mineral potential, and appearing on the terrain surface. The Northern area is characterized by a fault system that develops in the Northeast - Southwest direction. The tectonic activity here has also formed many positive anomalous clusters and has revealed many mineral spots on the surface. In the Eastern area, the geological structure is quite stable. The southeast and the South are characterized by a fault system developing in the sub-latitude direction, forming local heterogeneous blocks extending in the East-West direction.

The potential area of deep-hidden minerals (Figure 11) is determined by the maximum values of the horizontal gradient of the vertical derivative of the closed loop residual gravity anomaly field with amplitude > 0.007 mGal/m (Figure 9), combined with the residual gravity anomaly value (Figure 7), and exposed mineral spot locations on the surface (Figure 1b). The results of Figure 11 show that the majority of mineral prospect areas according to the residual potential anomaly field (orange) are mainly concentrated in the western, northwest, and southeast regions of the study area, these mineral prospects have revealed mineral spots on the topographic surface; some mineral prospects (yellow) have not yet revealed mineral spots on the topographic surface.

The results of zoning the mineral prospect area and identifying the hidden fault system buried by sediments (East and southeast of the study area) will provide geophysicists and geologists with detailed research plans to evaluate specific types of minerals in the Ba Na area.

4. Conclusions

The results of processing and interpreting potential field data in the Ba Na area give the following conclusions:

- The «live window» energy filter optimized the local anomaly information related to the deep-

hidden mineral location compared to the «fixed window» energy filter. The results of evaluating the high-frequency component of the magnetic anomaly field show shortcomings in the processing of aeromagnetic observations, and we have given an appropriate correction value before processing.

- The fault system includes the sub-latitude, sub-longitude, and northeast-southwest fault systems, in which the sub-latitude fault system is dominant. The eastern area (bordering the sea) is covered with sediments, according to the analysis results of the maximum horizontal gradient of the vertical derivative of the potential field, the fault systems have been identified that cannot be determined on the geological data.

- The area of mineral prospect according to the potential field anomaly is mainly concentrated in the western, northern, and southeastern areas of the study area, most of the promising mineral areas have exposed mineral spots on the terrain surface.

- The results of the analysis and interpretation of the potential field data provided Geophysicists and Geologists with detailed research plans to evaluate specific types of minerals in the Ba Na area.

Acknowledgements

The authors would like to thank the project of Ministry with code: TNMT.2022.02.20. We thank Pro.D.Sc. Petrov Alekcey Bladimirovich for supporting COSCAD 3D software, and at the same time would like to thank colleagues and reviewers for the time and support they have taken in reading and reviewing this paper.

Contribution of authors

Hong Thi Phan and Thong Duy Kieu - conceptualization, methodology, collected and synchronized data sources, processed data, interpreted processing results, and writing - review & editing; Phuong Minh Do - geological interpretation; Huu Van Tran - processing and interpretation of the results.

References

Blakely, R. J. (1996). *Potential theory in gravity and magnetic applications*. Cambridge University Press. 197 pages. https://www.cambridge.org/ core/books/ potential-theory-in-gravity-and-magnetic-applications/348880F23008 E16E66 3D6AD1 4A41D8DE.

Cordell, L. (1979). Gravimetric expression of graben faulting in Santa Fe country and the Espanola Basin, New Mexico. *In New Mexico Geological Society Guidebook, 30th Field Conference,* 59-64. https://www.scirp.org/(S(lz5mqp453edsnp55rrgjct55))/reference/ReferencesPapers.aspx?ReferenceID=1323561.

Fedi, M., and Florio, G. (2001). Detection of potential fields source boundaries by enhanced horizontal derivative method. *Geophysical prospecting*, 49(1): 40-58. https://doi.org/10.1046/j.1365-2478.2001. 00235.x.

Geosoft, (2008). Ver. 7.01: Manuals, Tutorials, and Technical Notes. Geosoft inc.

Hong, T. P., Petrov, A. V., Phuong, M. D., Luu, T. N. (2021). Geological region by multi-signal method of gravity anomaly data in central area of Vietnam. *Journal of Mining and Earth Sciences*, 62(5). 43-55. http://tapchi.humg.edu.vn/images/paper/2021/62_5/04.%20Phan%20Thi%20Hong%2043%20-%2054.pdf.

http://www.coscad3d.ru/index.php.

http://www.geosoft.com.

https://topex.ucsd.edu/cgi-bin/get_data.cgi.

https://www.generic mapping-tools.org/ download/.

https://www.ncdc.noaa.gov.

Nguyen, N. T., Bui, V. N., Nguyen, T. T. H. (2014). Determining the depth to the magnetic basement and fault systems in Tu Chinh - Vung May area by magnetic data interpretation. *Journal of Marine Science and Technology*. 14(4A). 16-25. DOI: 10.15625/ 1859-3097/14/4A/6027.

Nguyen, T. L. (2000a). Flight measured from the 1:50,000 scale gamma spectrum and 1: 100 000 scale gravity measurement in the central region of Vietnam. *Center for Information, Geological Archives,* Hanoi, 157 pages. (in Vietnamese).

Nguyen, X. S. (2000b). Flight results measured from 1: 50,000 scale gamma spectrum and measured in Kon Tum area. Center for Information*, Geological Archives*, Hanoi, 174 pages. (in Vietnamese).

Nikitin A. A., Petrov A. V., (2008). Theoretical foundations of geophysical information processing. *Science and Technology Publishing House*. Moscow, Russia, 127 pages. (in Russian) https://www.geokniga.org/bookfiles/geokniga-nikitinteorosnovygeofizinfo 2008.pdf.

Nikitin, A. A., Zinovkin, S. V, Petrov, A. V., Piskun, P. V. (2006). Adaptive techniques for identifying inhomogeneous geological objects in geophysical fields. *Geology and exploration,* UDK 550.834, no. 3, 50-56. (in Russian) https://elibrary.ru/item.asp?id=20781243.

Petrov, A. V. (2018). Adaptive processes handle the interpretation of non-permanent geographic fields in "KOSKAD-3D" computer technology. *International Scientific Conference*, April 1-2, MGRI-RGRU, Moscow, Russia, volume 1, 418-420. (in Russian) https://mgri.ru/science/scientific-practical-conference/2018-doc/tom1_compressed.pdf.

Petrov, A. V., Yudin, D. B., Soeli Hou, (2010). Processing and interpretation of geophysical data using a probabilistic-statistical approach using computer technology "KOSKAD 3D". *Earth science*. UDK 551-214, no. 2, 126-132. (in Russian) http://www.kscnet.ru/kraesc/ 2010 /2010_16/art13.pdf.

Phan, T. H., Petrov, A. V., Do, M. P. (2021). Application of the 2D filtering algorithm in the sliding window of the "living" form on the example of central Vietnam. *XV international scientific and practical conference "New ideas in the earth sciences"*, MGRI-RGGRU. volume 4, 339-343. https://mgri.ru/science/scientific-practical-conference/2021/%D0%A2%D0%BE%D0%BC%204.pdf.

Verduzco, B., Fairhead, J. D., Green, C. M., and MacKenzie, C. (2004). New insights into magnetic derivatives for structural mapping. *The Leading Edge*, 23(2), 116-119.https://doi.org/10.1190/1.1651454.